

The dynamics of sexual conflict over mating rate with endosymbiont infection that affects reproductive phenotypes

T. I. HAYASHI,* J. L. MARSHALL† & S. GAVRILETS*‡

*Department of Ecology and Evolutionary Biology, University of Tennessee, Knoxville, TN, USA

†Department of Entomology, Kansas State University, Manhattan, KS, USA

‡Department of Mathematics, University of Tennessee, Knoxville, TN, USA

Keywords:

coevolution;
maternal inheritance;
mathematical models;
reproductive traits;
sexual selection;
Wolbachia.

Abstract

Maternally inherited endosymbionts have been implicated as significant drivers of sexual conflict within their hosts, typically through sex-ratio manipulation. Empirical studies show that some of these endosymbionts have the potential to influence sexual conflict not by sex-ratio distortion, but by altering reproductive traits within their hosts. Research has already shown that reproductive traits involved in mating/fertilization process are integral 'players' in sexual conflict, thus suggesting the novel hypothesis that endosymbiont-induced changes in reproductive phenotypes can impact the dynamics of sexual conflict. Here, we use a standard quantitative genetic approach to model the effects of endosymbiont-induced changes in a female reproductive trait on the dynamics of sexual conflict over mating/fertilization rate. Our model shows that an endosymbiont-induced alteration of a host female reproductive trait that affects mating rate can maintain the endosymbiont infection within the host population, and does so in the absence of sex-ratio distortion and cytoplasmic incompatibility.

Introduction

Promiscuity is rampant among sexually reproducing organisms. Indeed, the long-held notion that females are sexually monogamous has been shattered by evolutionary biologists over the past few decades (reviewed in Birkhead, 2000). More generally, the idea that mating strategies are cooperative tactics to ensure successful fertilization has been replaced by the harsh reality that both males and females look to maximize their individual fitness relative to individuals of the *same* sex (Birkhead, 2000; Arnqvist, 2004; Arnqvist & Rowe, 2005). Consequently, alleles which enhance an individual's mating and fertilization success can spread in a population, even if they depress the average fitness of individuals in the population (Arnqvist, 2004). Therefore, alleles in one sex partly determine the individual fitness of alleles in the opposite sex. Such interplay between sex-specific alleles

provides the foundation for a coevolutionary arms race between the sexes that is antagonistic, with each successive counter-adaptation enhancing individual fitness relative to members of the same sex (Rice & Holland, 1997; Partridge & Hurst, 1998; Rice, 1998).

For example, male-specific alleles for high mating rate typically have higher fitness than low mating rate alleles, even though high mating rates can negatively impact the fitness of a female (e.g. Arnqvist & Nilsson, 2000; Maklakov *et al.*, 2005). In this scenario, female-specific resistance-to-mating alleles would be under positive selection to reduce the costs of mating (e.g. polyspermy and caustic seminal fluid proteins; Chapman *et al.*, 1995; Civetta & Clark, 2000). With the spread of such female-specific alleles, males would once again be under selection for higher mating rates, thus perpetuating the antagonistic coevolution. This type of sexual conflict has been suggested as a general cause of continuous and rapid coevolution of reproductive traits (reviewed in Rice & Holland, 1997; Holland & Rice, 1998; Rice, 1998; Chapman *et al.*, 2003; Pizzari & Snook, 2003; Arnqvist & Rowe, 2005). Moreover, theoretical models have shown that sexual conflict over mating rate can drive rapid,

Correspondence: Takehiko I. Hayashi, Research Center for Chemical Risk Management, National Institute of Advanced Industrial Science and Technology, 16-1 Onogawa, Tsukuba, Ibaraki 305-8589, Japan.
Tel.: +81 29 861 8771; fax: +81 29 861 8904;
e-mail: ti-hayashi@aist.go.jp

antagonistic coevolution in reproductive traits (reviewed in Gavrillets & Hayashi, 2005).

Manipulations of sex ratio can also influence the dynamics of sexual conflict, as female-biased sex ratios are believed to dampen sexual conflict via a reduction in polyandry (see Arnqvist & Rowe, 2005). For this reason and others, female-biasing, sex-ratio distorters (like some strains of the reproductive endosymbiont *Wolbachia*) are thought to have profound effects on host reproductive biology (e.g. Weeks *et al.*, 2002; Rigaud & Moreau 2004; Wernegreen, 2004; Zeh & Zeh, 2005). Therefore, it is clear that sex-ratio-distorting endosymbionts can influence sexual conflict over mating rate simply by changing the sex ratio.

Interestingly, a few empirical studies have shown that *Wolbachia*, in the absence of sex-ratio distortion, can alter reproductive phenotypes that may affect mating (or fertilization) rate. For example, Wade & Chang (1995) show that *Wolbachia* infections can increase the competitiveness of sperm in the flour beetle *Tribolium*. More recently, Marshall (2007) shows that *Wolbachia* can alter the length of the female reproductive tract in the ground cricket *Allonemobius*. Specifically, Marshall (2007) found that: (1) there is a *Wolbachia* infection-by-population interaction effect on the length of the spermathecal duct; (2) the infection-induced modification on spermathecal duct length appears to be caused by *Wolbachia* and not another bacterium; and (3) experimental curing of *Wolbachia* in juvenile females recovers the uninfected adult morphology. Both of the above *Wolbachia*-induced modifications could potentially affect fertilization rate – thus suggesting a novel role for endosymbionts in sexual conflict. However, it is still not clear why these reproductive traits are influenced by *Wolbachia*. One possibility is that the endosymbiont may gain fitness benefits (e.g. maintenance of infection) by influencing sexual conflict over mating/fertilization rate. The endosymbiont-induced altering of the reproductive quantitative trait rather than sex ratio can significantly affect the dynamics of sexual conflict. The ubiquity of reproductive endosymbionts in arthropods (e.g. Werren & Windsor, 2000) suggests that the novel mechanism may potentially be present in a broad range of species. Given its potential importance, we wanted to assess the dynamics of sexual conflict over mating/fertilization rate when endosymbiont infections affect reproductive phenotypes, not sex ratio.

Here, we develop a model of sexual conflict over mating (or fertilization) rate when an endosymbiont infection alters a female phenotype that affects the mating (or fertilization) rate. As suggested by empirical studies (e.g. Arnqvist & Nilsson, 2000; Maklakov *et al.*, 2005) and often assumed in models of sexual conflict over mating rate (reviewed in Gavrillets & Hayashi, 2005), we assume that male fitness increases with increased mating rate whereas female fitness is optimized at an intermediate mating rate because of various costs of reproduction (reviewed in Arnqvist & Rowe, 2005). We

use a standard quantitative genetic approach (e.g. Lande 1976, 1979; Iwasa *et al.*, 1991; Gavrillets 1997) which has previously been successfully applied to modelling sexual conflict (e.g. Gavrillets, 2000; Gavrillets *et al.*, 2001; Gavrillets & Hayashi, 2006). The objectives of this study were to: (i) examine whether the endosymbiont-induced alteration of host female phenotype could be adaptive for the endosymbiont; and (ii) study the possible evolutionary impact of endosymbiont infection on the reproductive traits involved in sexual conflict over mating rate.

Model

Reproductive interactions between sexes are mediated by two independent, sex-limited quantitative traits: a female (egg) trait X and a male (sperm) trait Y (see Table 1 for a glossary of notation). Motivated by Marshall's (2007) study of the *Wolbachia*-induced alteration of female phenotype in the *Allonemobius socius* complex of ground crickets, we assume that: (1) the endosymbiont infection only affects females (i.e. there is no induced phenotype or direct cost of harbouring the endosymbiont for males) and is transmitted only maternally (i.e. mother to daughter) with probability $1 - \mu$, where $0 \leq \mu < 1$ is the probability of infection loss during transmission; (2) the endosymbiont infection increases female phenotype by a value c taken from a probability distribution $h(c)$ with mean value \bar{c} ; and (3) there is no other phenotypic effect caused by the endosymbiont infection. The phenotypes of uninfected and infected females, respectively, are given by $X = x + e_x$ and $X = x + c + e_x$, where x and e_x are genotypic and microenvironmental effects on the female phenotype, respectively, and c is the phenotypic alteration by the infection. The male trait is given by $Y = y + e_y$, where y and e_y are genotypic and microenvironmental effects respectively. The distributions of x and y in the population are denoted as $f(x)$ and $g(y)$ with mean values \bar{x} and \bar{y} respectively. The probability distributions of e_x and e_y are denoted as $m(e_x)$ and $n(e_y)$ with means equal to zero. We assume that y , e_y , x , e_x and c are independent.

Let $\Psi(X, Y)$ be the probability that mating (or fertilization) between female X and male Y is not prevented by an isolating mechanism. Below, we will refer to $\Psi(X, Y)$ as 'compatibility'. The proportion of males compatible with females X is

$$P(X) = \iint \Psi(X, y + e_y)g(y)n(e_y)dyde_y. \quad (1)$$

The proportion of females compatible with male Y is

$$Q(Y) = p \iiint \Psi(x + c + e_x, Y)f(x)h(c)m(e_x)dx dc de_x \\ + (1 - p) \iint \Psi(x + e_x, Y)f(x)m(e_x)dx de_x, \quad (2)$$

where p is the frequency of infected female ($0 \leq p \leq 1$). We regard $P(X)$ and $Q(Y)$ as the proxies of female and

Table 1 Glossary of notations.

X	female (or egg) phenotype
x	genotypic effect in female (or egg) phenotype
$f(x)$	distribution of x
\bar{x}	mean of x
V_x	variance of x
\bar{X}	mean of X , defined as $\bar{X} = p(\bar{x} + \bar{c}) + (1 - p)\bar{x}$
Y	male phenotype
\bar{Y}	mean of Y
y	genotypic effect in male (or sperm) phenotype
\bar{y}	mean of y
$g(y)$	distribution of y
V_y	variance of y
c	increase in female phenotype by infection
$h(c)$	probability distribution of c
\bar{c}	mean of c
e_x	environmental effect in female (or egg) phenotype
$m(e_x)$	probability distribution of e_x
e_y	environmental effect in male (or sperm) phenotype
$n(e_y)$	probability distribution of e_y
p	frequency of infected female, $0 \leq p \leq 1$
z	difference between sexes traits, given by $z = x - y$
\bar{z}	difference between average sexes traits, given by $\bar{z} = \bar{x} - \bar{y}$
$\Psi(X, Y)$	compatibility between female having X and male having Y
$P(X)$	proportion of males that would be compatible with female having X
$Q(Y)$	proportion of females that would be compatible with male having Y
W_I	fitness of infected female
W_U	fitness of uninfected female
W_m	fitness of male
Ψ_I	compatibility of infected female evaluated at $x = \bar{x}$ and $y = \bar{y}$
Ψ_U	compatibility of uninfected female evaluated at $x = \bar{x}$ and $y = \bar{y}$
$\bar{\Psi}$	average compatibility, given by $\bar{\Psi} = p\Psi_I + (1 - p)\Psi_U$
Ψ_{xI}	derivative of with respect to x
Ψ_{yI}	derivative of Ψ_I with respect to y
Ψ_{xU}	derivative of Ψ_U with respect to x
Ψ_{yU}	derivative of Ψ_U with respect to y
α	range of compatibility between x and y (α is inversely related to the range)
μ	fraction of uninfected ova produced by an infected female transmission rate is defined as $1 - \mu$
P_{opt}	optimal mating rate for female
a	strength of selection by sexual conflict in females
b	fitness gain of male by increasing mating rate
s_x	strength of stabilizing natural selection to x (or X)
s_y	strength of stabilizing natural selection to y (or Y)
θ_x, θ_y	optimum of x and y with respect to natural selection, respectively
s_c	cost of being infected for females that is independent of their phenotype
S_I	average cost (for infected females) caused by endosymbiont infection

male mating (or fertilization) rates. Female fitness increases with $P(X)$ at small mating rates (because with increased mating comes an increased probability of successful fertilization). However, high mating rates become damaging to females (reviewed in Arnqvist &

Rowe, 2005). Therefore, female fitness is optimal at intermediate values of $P(X)$. Following previous work (e.g. Gavrillets, 2000; Gavrillets *et al.*, 2001; Gavrillets & Waxman, 2002), we postulate that female fitness is given by a quadratic function of $P(x)$:

$$W_{f,sex}(X) = 1 - a[P(X) - P_{opt}]^2, \quad (3)$$

where P_{opt} ($0 < P_{opt} < 1$) is an optimal value and a is a measure of how important it is for females to succeed in optimizing their mating rates. By contrast, male fitness should be a monotonically increasing function of their mating rate $Q(Y)$. We use the simple linear function

$$W_{m,sex}(Y) = 1 + 2bQ(Y), \quad (4)$$

where b is a positive parameter measuring the intensity of sexual selection on males (and the constant 2 is merely for mathematical convenience). Larger values of a and b imply stronger selection in females and males respectively.

Finally, we assume direct natural selection on both traits. We consider two possibilities. First, natural selection can act directly on phenotypes X and Y . To describe the corresponding fitness components of infected females ($W_{I,nat}$), uninfected females ($W_{U,nat}$) and males ($W_{m,nat}$), we use the quadratic functions:

$$W_{I,nat}(x) = [1 - s_x(x + c + e_x - \theta_x)^2](1 - s_c), \quad (5a)$$

$$W_{U,nat}(x) = 1 - s_x(x + e_x - \theta_x)^2 \text{ and} \quad (5b)$$

$$W_{m,nat}(y) = 1 - s_y(y + e_y - \theta_y)^2. \quad (5c)$$

Parameters s_x and s_y measure the strength of natural selection, whereas parameters θ_x and θ_y specify optima under natural selection for the traits. Parameter s_c is the cost of being infected that is independent of the host female phenotype.

Second, selection can act directly on genotypic values (i.e. x and y). For example, the endosymbiont may produce an enzyme that results in an increase in female phenotype without demanding *extra* energetic investment for host females. (In other words, an endosymbiont may enable host females having genetic value x to increase her phenotype to $x + c$ with the same energetic cost required for her to develop her phenotype to x when uninfected.) Then, if the energetic cost is the focal factor for natural selection on the female trait, selection acts on the amount of latent energetic investment (x), not on the realized phenotype (X). This case is described by fitness functions for infected females ($W_{I,nat}$), uninfected females ($W_{U,nat}$) and males ($W_{m,nat}$) as follows:

$$W_{I,nat}(x) = [1 - s_x(x - \theta_x)^2](1 - s_c), \quad (6a)$$

$$W_{U,nat}(x) = 1 - s_x(x - \theta_x)^2 \text{ and} \quad (6b)$$

$$W_{m,nat}(y) = 1 - s_y(y - \theta_y)^2. \quad (6c)$$

Note that the case of directional selection on a trait can be incorporated by assuming that the corresponding optimum is at a boundary of possible trait values (e.g. at zero).

Throughout the paper, we will use a standard weak selection approximation assuming parameters a , b , s_x , s_y and s_c are small and that the function changes weakly over the range of males and females present in the population (see Iwasa *et al.*, 1991; Gavrillets, 2000 and Gavrillets *et al.*, 2001 for an explanation of mathematical techniques used). The fitnesses of infected females ($W_I(x)$), uninfected females ($W_U(x)$) and males ($W_m(y)$) are approximated as

$$W_I(x) = \{1 - a[\Psi(x + \bar{c}, \bar{y}) - P_{\text{opt}}]^2\} W_{I,\text{nat}}(x), \quad (7a)$$

$$W_U(x) = \{1 - a[\Psi(x, \bar{y}) - P_{\text{opt}}]^2\} W_{U,\text{nat}}(x) \quad \text{and} \quad (7b)$$

$$W_m(y) = \{1 + 2b[p\Psi(\bar{x} + c, y) + (1 - p)\Psi(\bar{x}, y)]\} W_{m,\text{nat}}(y). \quad (7c)$$

Note that the effects of variances and higher moments of x , y , c , e_x and e_y are negligible under the weak selection approximation.

Our model assumes that infection is only inherited from mother to daughter (Werren, 1997). The frequency of infected females in the next generation depends on the fitness of infected females relative to the average fitness of all females in the population (cf. Hoffmann *et al.*, 1990; Turelli *et al.*, 1992; Turelli, 1994). When natural selection acts on the genotypic values (x and y), the average fitness of infected females (\bar{W}_I), uninfected females (\bar{W}_U), and all females in populations (\bar{W}_f) are approximated as

$$\bar{W}_I = 1 - a[\Psi(\bar{x} + \bar{c}, \bar{y}) - P_{\text{opt}}]^2 - S_I - s_x(\bar{x} - \theta_x)^2, \quad (8a)$$

$$\bar{W}_U = 1 - a[\Psi(\bar{x}, \bar{y}) - P_{\text{opt}}]^2 - s_x(\bar{x} - \theta_x)^2 \quad \text{and} \quad (8b)$$

$$\bar{W}_f = p\bar{W}_I + (1 - p)\bar{W}_U, \quad (8c)$$

where S_I is the average fitness cost for infected females caused by the infection, which is given by $S_I = s_c$. When natural selection acts on the phenotypes (X and Y), S_I is given by $S_I = s_c + s_x\bar{c}[2(\bar{x} - \theta_x) + \bar{c}]$. In the derivation of eqns (8a)–(8c), the terms with products of a , b , s_x , s_y and s_c are negligible under weak selection approximation.

When natural selection acts on the genotypic values (x and y), the dynamic equations for changes in the mean trait values and infection frequency between two subsequent generations are

$$\Delta\bar{x} = V_x\{a[p(P_{\text{opt}} - \Psi_I)\Psi_{xI} + (1 - p)(P_{\text{opt}} - \Psi_U)\Psi_{xU}] - s_x(\bar{x} - \theta_x)\}, \quad (9a)$$

$$\Delta\bar{y} = V_y\{b[p\Psi_{yI} + (1 - p)\Psi_{yU}] - s_y(\bar{y} - \theta_y)\} \quad \text{and} \quad (9b)$$

$$\Delta p = p\{(1 - p)[a(\Psi_U - \Psi_I)(\Psi_U + \Psi_I - 2P_{\text{opt}}) - S_I] - \mu\}, \quad (9c)$$

where V_x and V_y are the additive genetic variances of x and y . Ψ_I and Ψ_U are the average compatibilities of infected and uninfected females with males, which are given by $\Psi_I = \Psi(\bar{x} + \bar{c}, \bar{y})$ and $\Psi_U = \Psi(\bar{x}, \bar{y})$ respectively. Ψ_{xI} and Ψ_{yI} are evaluated at $X = \bar{x} + \bar{c}$ and $Y = \bar{y}$, whereas Ψ_{xU} and Ψ_{yU} are evaluated at $X = \bar{x}$ and $Y = \bar{y}$ (the subscripts x and y denote the derivatives with respect to x and y respectively). Note that assuming weak selection implies that linkage disequilibrium is negligible and we assume that genetic covariance between male and female traits is absent. In the derivation of eqn (9c), it is straightforward to show from eqn (8c) that $\Delta p = p[(1 - p)(W_I - W_U)/W_f - \mu W_I/W_f]$. A first-order approximation, ignoring the expressions of order a^2 and $a\mu$, leads to eqn (9c). When natural selection acts on the phenotypes (X and Y), the last term in the right-hand side of eqn (9a) is $s_x(\bar{x} - \theta_x + p\bar{c})$ instead of $s_x(\bar{x} - \theta_x)$. Note that assuming $p = 0$ (i.e. assuming no infection) results in the same equations as eqns 4a,b in Gavrillets *et al.* (2001).

Analysis of the dynamics of infection frequency

The difference in the frequency p of infected females between subsequent generations is given by eqn (9c) and can also be rewritten as

$$\Delta p = p[(1 - p)(\bar{W}_I - \bar{W}_U) - \mu]. \quad (10)$$

We can derive some basic results from eqns (9c) and (10). The equilibrium infection frequency (p^*) can be found from the equation

$$p^* = 1 - \frac{\mu}{\bar{W}_I^* - \bar{W}_U^*} \quad (11a)$$

$$= 1 - \frac{\mu}{a(\Psi_U^* - \Psi_I^*)(\Psi_U^* + \Psi_I^* - 2P_{\text{opt}}) - S_I}, \quad (11b)$$

where the asterisk means that the values are computed at equilibrium. Maintaining infection is possible if

$$\bar{W}_I^* - \bar{W}_U^* > \mu, \quad (12)$$

that is, if the difference in fitness between infected and uninfected females is larger than the probability of infection loss at the equilibrium. The inequality (12) can also be rewritten as

$$a(\Psi_U^* - \Psi_I^*)(\Psi_U^* + \Psi_I^* - 2P_{\text{opt}}) > \mu + S_I. \quad (13)$$

Equations (11b) and (13) show that an increase in the rate of transmission loss (μ), the average cost of being infected (S_I) or optimal mating rate for females (P_{opt}) decreases the equilibrium infection frequency. Increase in the strength of selection by sexual conflict in females (a) increases the equilibrium infection frequency. The maintenance of infection also requires that the average compatibility of uninfected females with males be higher than that of infected females (i.e. $\Psi_U^* > \Psi_I^*$). Note that $\Psi_U^*, \Psi_I^* > P_{\text{opt}}$ is almost always satisfied because neither females nor males favour mating rates that are less than

the female optimum. If a phenotype is not induced by the endosymbiont infection (i.e. $c = 0$), then the inequality in eqn (13) is not satisfied (and thus infection cannot be maintained) because $c = 0$ means $\Psi_U = \Psi_I$. The above results for infection frequencies do not depend on particular forms of functions for fitness and compatibility between the sexes.

Dynamics with quadratic compatibility function

First, we analysed the dynamic equations assuming a quadratic compatibility function, $\Psi(X, Y) = 1 - \alpha(Y - X)^2$ (cf. Gavrillets, 2000), where parameter α controls the range of compatibility between X and Y . The values of α must be chosen so that $\Psi(X, Y) > 0$ within the ranges of X and Y . This function may be applicable if mating or fertilization probability depends on 'matching' between female and male phenotypes.

No infection

When there is neither infection (i.e. $p = 0$) nor natural selection (i.e. $s_x = s_y = 0$), the eqns (9a)–(9c) are the same as eqns 4a,b in Gavrillets (2000) (except for the notation system). As a baseline for the cases with infection, we briefly describe results for cases without infection. Gavrillets (2000) showed that there are two qualitatively different outcomes. First, if sexual selection on males is sufficiently strong relative to that on females [precisely, $bV_y > (1 - P_{\text{opt}})aV_x$], the population evolves toward a line satisfying $\bar{x} = \bar{y}$ (Fig. 1 in Gavrillets, 2000). Subsequent changes in trait values along the line $\bar{x} = \bar{y}$ can be caused by neutral drift. Second, if sexual selection on males is not sufficiently strong relative to that on females [precisely, $bV_y < (1 - P_{\text{opt}})aV_x$], then continuous coevolution (i.e. continuous changing of the average trait values of females and males) occurs between sexes (Fig. 2 in Gavrillets, 2000). During coevolution, the difference in the mean trait values, $\bar{z} = \bar{y} - \bar{x}$, approaches asymptotically a constant value displaced from zero. The value of the displacement (\bar{z}) is intermediate between those that are optimal for males (zero displacement) and females (displacement at a value of P_{opt}). Our numerical analysis suggests that the incorporation of natural selection on the traits of each sex results in an evolution towards stable equilibria (data not shown).

Infection but no natural selection

When there is no natural selection on the traits (i.e. $s_x = s_y = 0$), the dynamics with infection (i.e. the case when p can be positive) results in one of the three qualitatively different outcomes. First, endosymbiont infection cannot be maintained when inequalities (12) and (13) are not satisfied under the realized value of displacement \bar{z} . For example, Fig. 1 shows that infection always disappears (i.e. p becomes zero) whenever $\bar{z} > \bar{c}/2$. This is because the average male trait is

always more compatible with infected females than uninfected females when $\bar{z} > \bar{c}/2$. Similarly, infection is not maintained when $|\bar{z}|$ is too large. For example, suppose that $|\bar{z}|$ is large enough to satisfy $\Psi_U = P_{\text{opt}}$. In this case, infection cannot be maintained because any deviation in the phenotype causes suboptimal mating rate. Once the infection disappears (i.e. $p = 0$), the system degenerates to the case without infection discussed above.

The second outcome is coevolution between x and y to a line of equilibria while maintaining infection (Fig. 1a–c). This outcome requires that: (1) sexual selection on males is sufficiently strong relative to that on females (precisely, $bV_y > (1 - P_{\text{opt}})aV_x$; see Appendix for detail); (2) initial values allow for maintenance of infection during coevolution to the line of equilibria; and (3) the inequality $\bar{W}_I - \bar{W}_U > \mu$ (eqn 12) is satisfied at equilibrium. Our numerical simulations show that coevolution between x and y stops in the neighborhood of the value of \bar{z} that satisfies $\bar{y} = \bar{X}$ (Fig. 1a–c). This means that the equilibrium value of the displacement \bar{z} depends on the infection frequency p (because $\bar{y} = \bar{X} = (1 - p)\bar{x} + p(\bar{x} + \bar{c}) = \bar{x} + p\bar{c}$ and thus $\bar{z} = p\bar{c}$). The average male phenotype is always located between the average phenotypes of uninfected (\bar{x}) and infected ($\bar{x} + \bar{c}$) females. The equilibrium frequency of p cannot be larger than 0.5 because infection always disappears whenever $\bar{z} > \bar{c}/2$ [$\bar{z} > \bar{c}/2$ does not satisfy inequality (13)]. The average compatibility ($\bar{\Psi}$) is intermediate between the optimum values for males and females (i.e. between one and P_{opt}) (Fig. 1c).

The third outcome is continuous coevolution between males and females while maintaining infection (Fig. 1d–f). During coevolution, the difference in the mean trait values between the sexes (\bar{z}) and infection frequency (p) approach asymptotically constant values which satisfy $|\bar{z}| \leq \{[P_{\text{opt}} + (bV_y/aV_x) - 1]/\alpha\}^{1/2} \leq |\bar{z} - \bar{c}|$ (Fig. 1e,f; see Appendix for an analysis). Note that \bar{z} and \bar{c} always have opposite signs in this outcome. p determines the asymptotic value of \bar{z} within the above range. This outcome requires that: (1) sexual selection on males is not sufficiently strong relative to that on females (precisely, $bV_y < (1 - P_{\text{opt}})aV_x$; see Appendix for detail); (2) initial values allow for the maintenance of infection during coevolution; and (3) the resulting displacement \bar{z} satisfies $\bar{W}_I - \bar{W}_U > \mu$ (inequality 12).

The equilibrium infection frequency decreases with increasing s_c ($=S_I$), as shown in eqn (9b). Note that the presence of the cost of being infected (i.e. $s_c > 0$) does not mean that infection cannot be maintained. The maintenance of infection is possible as long as the cost is small enough to satisfy inequality (13).

Infection and natural selection

When natural selection acts on the genotypic values (x and y), whether or not an endosymbiont infection is maintained largely depends on the equilibrium value of

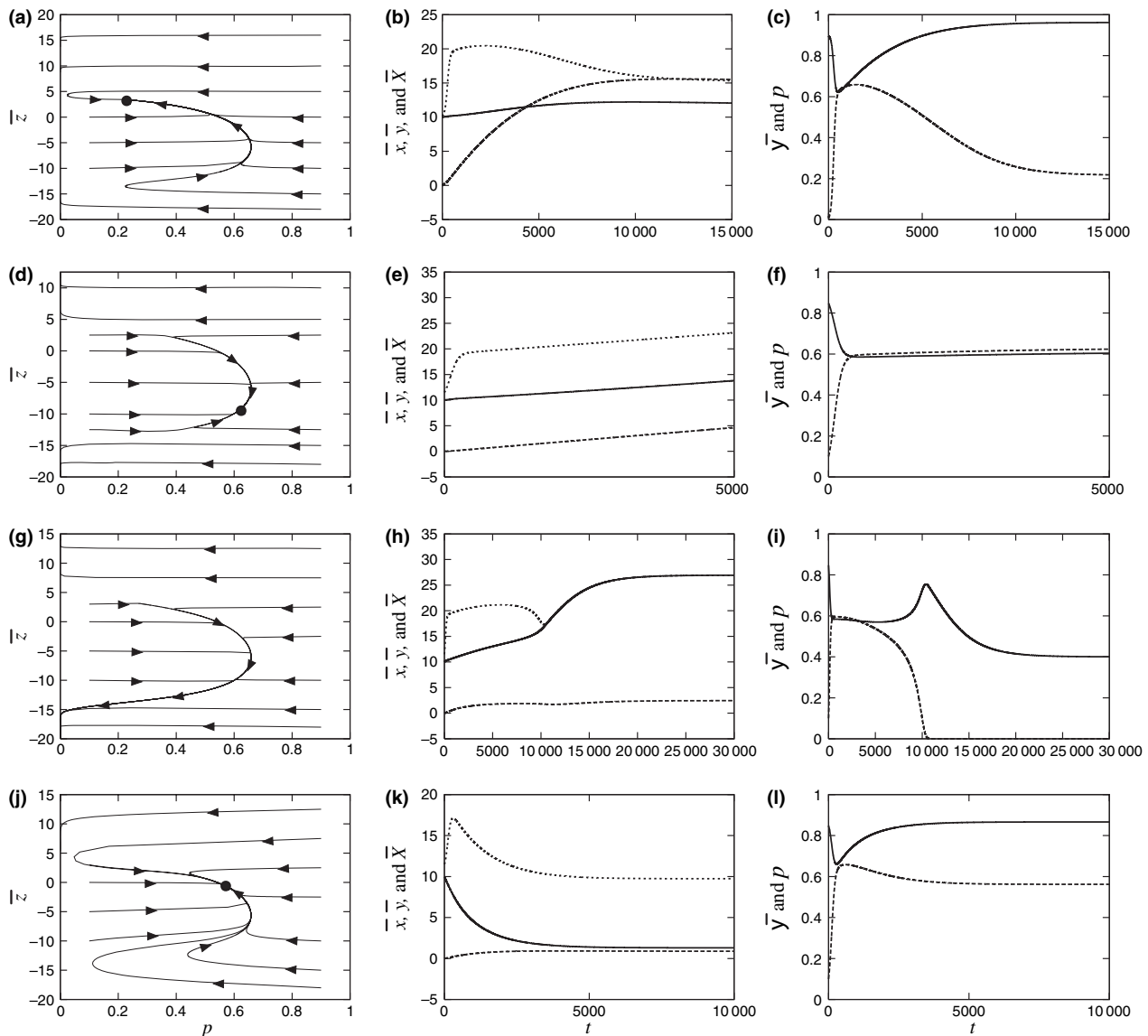


Fig. 1 The dynamics of infection frequencies (p), average female (\bar{x}) and male (\bar{y}) genotypic values and the displacement ($\bar{z} = \bar{x} - \bar{y}$) under a quadratic compatibility function. (a–c) Evolution towards a line of equilibria while maintaining infection ($V_x = 0.5$, $V_y = 2$, $a = 0.1$, $b = 0.05$, $\bar{c} = 15$, $\mu = 0.01$, $\alpha = 0.001$, $P_{\text{opt}} = 0.4$, $s_x = 0$, $s_y = 0$, $s_c = 0$, $\theta_x = 0$, $\theta_y = 0$). (d–f) Continuous coevolutionary chase while maintaining infection (parameters are the same as in (a–c) but with $V_x = 2$ and $V_y = 0.5$). (g–i) The elimination of infection under natural selection on genotypic values in male only (parameters are the same as in (a–c) but with $s_y = 0.001$). (j–l) The maintenance of infection under direct natural selection on genotypic values (parameters are the same as in (a–c) but with $s_x = 0.0005$, $s_y = 0.001$). (a, d, g, j) The dynamics on the (p , \bar{z}) phase plane. Equilibrium points are specified with black circle. (b, e, h, k) Examples of the dynamics of \bar{x} (solid line), \bar{y} (dashed line) and \bar{X} (dotted line) in time. (c, f, i, l) Examples of the dynamics of average compatible rate $\bar{\Psi}$ (solid line) and p (dashed line) in time.

\bar{z} . In general, infection is less likely to be maintained when natural selection is stronger on males than females. For example, our numerical simulations show that if natural selection acts on males only, infection is likely to be eliminated (Fig. 1g–i). In this case, $|\bar{z}|$ typically increases until the optimal mating rate for females is reached and the fitness advantage of the endosymbiont-

induced phenotype eventually disappears. Then, the infection is not maintained because of the continuous decrease in the infection frequency because of incomplete transmission.

On the other hand, increasing natural selection on females enhances the maintenance of infection (Fig. 1j–l). In this case, natural selection on females tends to stop

coevolution at a point that nearly satisfies $\bar{z} = 0$, where males can be viewed as the winners of the sexual conflict. In such a situation, the endosymbiont-induced phenotype can improve the fitness of an infected female by reducing her mating rate and thus can lead to the maintenance of infection (Fig. 1j–l). The effect of s_c on the evolutionary dynamics is qualitatively the same as those in the cases without natural selection mentioned above.

When natural selection acts on the phenotype of females (X), our numerical simulations show that the maintenance of infection does not occur (unless μ is very close to zero, say, in the order of 10^{-3} or smaller). In this case, the cost of increasing the phenotype by being infected is the same as that by evolving an increase in the genotypic component x . Given the same cost, only the evolution of x lasts and the infection is not maintained because of the continuous decrease in the infection frequency because of the incomplete transmission.

Dynamics with S-shaped compatibility function

Here, we assume that the compatibility $\Psi(X, Y)$ is an S-shaped function of the difference $z = y - x$ between the male trait (stimulus) and female trait (resistance), such that $\Psi(X, Y) = 0$ for $z \rightarrow -\infty$, $\Psi(X, Y) = 1/2$ for $z = 0$ and $\Psi(X, Y) = 1$ for $z \rightarrow \infty$. (In numerical simulations below, $\Psi(X, Y) = \{\tanh[\alpha(Y - X)] + 1\}/2$.) Such a function may be applicable when an increase in male

phenotype stimulates female mating behaviour (or fertilization) and an increase in female phenotype enhances her resistance to the male's stimulation (cf. Gavrillets *et al.*, 2001).

When there is no natural selection, there are two qualitatively different outcomes. First, infection is not maintained in the population when: (1) $\bar{W}_I - \bar{W}_U \leq \mu$ for the current value of displacement \bar{z} ; or (2) sexual selection on males is sufficiently strong relative to that on females (precisely, $bV_y > (1 - P_{\text{opt}})aV_x$; see *Appendix* for detail) (Fig. 2a–c). Note that an S-shaped function does not result in the maintenance of infection at a line of equilibrium, which is observed in the case using a quadratic function (Fig. 1a–c). The second outcome is continuous evolution between x and y while maintaining infection (Fig. 2d–f), which is qualitatively similar to one of the outcomes with quadratic function (Fig. 1d–f). This outcome happens when sexual selection on males is not sufficiently strong relative to that on females (precisely, $bV_y < (1 - P_{\text{opt}})aV_x$; see *Appendix* for detail) and the resulting \bar{z} satisfies $\bar{W}_I - \bar{W}_U > \mu$ (inequality 12). Effects of natural selection on the reproductive traits are qualitatively the same as those under the dynamics with quadratic function (data not shown).

Discussion

Our model demonstrates that endosymbiont infections can be maintained within populations by modifying host

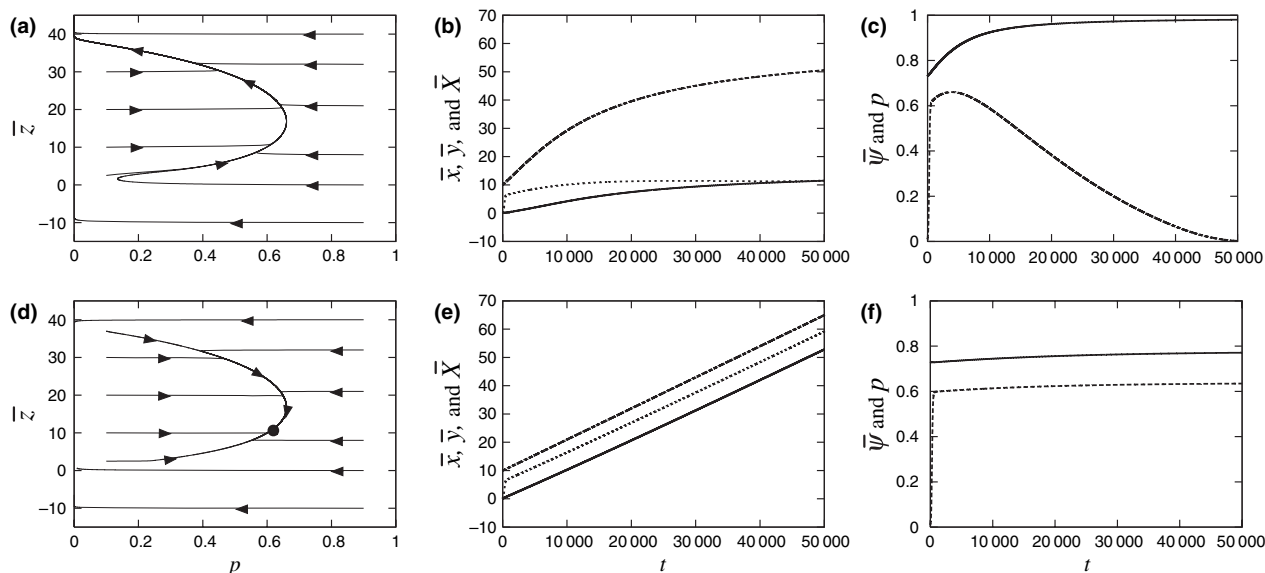


Fig. 2 The dynamics under an S-shaped compatibility function. (a–c) The disappearance of infection as the result of male winning coevolutionary chase (parameter values are the same as in Fig. 1a–c but with $\alpha = 0.05$ and $P_{\text{opt}} = 0.2$). (d–f) Continuous coevolutionary chase while maintaining infection (parameter values are the same as in (a–c) but with $V_x = 1.5$ and $V_y = 1$). (a, d) the dynamics on the (p, \bar{z}) phase plane. Equilibrium points are specified with black circle. (b, e) Examples of the dynamics of \bar{x} (solid line), \bar{y} (dashed line) and \bar{X} (dotted line) in time. (c, f) Examples of the dynamics of average compatible rate $\bar{\Psi}$ (solid line) and p (dashed line) in time.

female traits involved in sexual conflict over mating or fertilization rate. Specifically, the model shows that the phenotypic alteration by the endosymbiont can increase the fitness of its host females by decreasing the average compatibility with males within the population. This fitness advantage to infected host females enhances the maintenance of endosymbiont infection. Within our model (in which no sex-ratio distortion nor cytoplasmic incompatibility was present), endosymbiont infections can be maintained in three different ways. First, infections can be maintained during continuous coevolution between male and female reproductive traits. Secondly, infections can be maintained at equilibrium where the average male phenotype matches the average female phenotype. Thirdly, when natural selection acts not on the female phenotype but directly on genotypic values, infections can be maintained when the coevolution between the sex traits ends at an equilibrium – i.e. at a point where the phenotypic alteration provides a large enough advantage to infected females.

Our model also points to some important factors and parameters regarding infection dynamics. First, the outcome of infection dynamics largely depends on initial values. This suggests that whether or not infection can be maintained is determined not only by the biological properties of endosymbionts but also by the history and state of sexual conflict in each population. Secondly, the qualitative dynamics of coevolution between the genetic components of sex-specific traits (i.e. x and y) is largely independent of infection frequency, and instead depends on the genetic variances of the traits and the strength of sexual conflict and natural selection on the traits. Specifically, whether continuous coevolution occurs or not depends on the sign of the expression $bV_y - (1 - P_{\text{opt}})aV_x$, which does not include terms with infection frequency p . Thirdly, the equilibrium frequency of infected females increases with increasing strength of sexual conflict (i.e. decreasing P_{opt}). Because increasing the population size often increases the strength of sexual conflict (Gavrilets, 2000; Martin & Hosken, 2003), this predicts that infection frequency should positively correlate with population size. The equilibrium frequency of infected females also increases with increasing transmission rates and decreasing costs of being infected.

Another feature of our model is that infection can be maintained at equilibrium when the average male phenotype (\bar{Y}) is 'trapped' between the infected and uninfected phenotypes of the female (i.e. $\bar{x} < \bar{Y} < \bar{x} + \bar{c}$; Fig. 1a–c). This outcome appears similar to the Buridan's Ass regime (Gavrilets & Waxman, 2002), which is characterized by the extensive diversification in female traits and no corresponding diversification in male traits. In the model of Gavrilets & Waxman (2002), females diverge into two distinct clusters, whereas males are 'trapped' at the centre of the diverged female clusters. In the model presented here, two clusters (or a bimodal distribution) in female phenotype are created by the

infected and uninfected female phenotypes. As in the Buridan's Ass regime, the male phenotype is 'trapped' at the average phenotype of all females while the average mating rate is reduced by the variance in female phenotype.

As for empirical data, *Wolbachia* is often suggested as a cause of rapid speciation in host species (e.g. Shoemaker, 1999; Rokas, 2000; Bordenstein *et al.*, 2001; Wade, 2001). Our model suggests that phenotypic alterations induced by such endosymbionts can also be a force of speciation. Our model shows that trajectories and equilibrium values of coevolutionary dynamics depend on the degree of phenotypic alteration by the endosymbiont (i.e. the value of \bar{c}). For example, suppose that we change parameter \bar{c} from 15 to -15 while all else remains the same, as in the examples of Fig. 1. In this case, we will obtain the same dynamics on the (\bar{p}, \bar{z}) phase plane as Fig. 1a,d,g,j (because of the symmetry about $x-y$ in the model), but the sign of \bar{z} is reversed. This sign reversal corresponds to the changes in the direction of coevolutionary trajectories and the location of each equilibrium. This dependency of trajectories and equilibrium values on the degree of phenotypic alteration (\bar{c}) suggests that two identical populations can diverge in reproductive traits because of infection by different endosymbiont strains that have different phenotypic effects (i.e. different values of \bar{c}). This divergence could cause reproductive isolation between the populations, thus suggesting a novel mechanism for speciation via endosymbiont infection.

The maintenance of infection during continuous evolutionary chase may seem unrealistic given the assumption of unlimited phenotypic/genotypic space for female and male traits. One of the realistic outcomes of such continuous coevolution would be that stabilizing natural selection eventually stops the coevolutionary chase. Our models with stabilizing natural selection apply to these cases. If there is a boundary to the phenotypic/genotypic space and no natural selection, continuous evolutionary chase would eventually reach the boundary. Whether the infection is maintained or not would depend on the resulting value of \bar{z} at the boundary (i.e. whether the value of \bar{z} satisfies inequality (12) or not).

As we stated above, our model is also applicable to sexual conflict over fertilization compatibility as well as that over mating compatibility. For example, traits X and Y can be interpreted as an 'egg/reproductive tract trait' and 'sperm trait', respectively, whereas function $\Psi(X,Y)$ can be interpreted as 'fertilization probability'. It is this application of our model that fits the empirical data outlined in Marshall (2007), as the female trait (X) is the length of the female reproductive tract. However, it remains to be seen if the dynamics of *Wolbachia* infection in the *A. socius* system (Marshall, 2004, 2007) meets the predictions outlined by our model.

Overall, our results provide theoretical support to the verbal argument that endosymbiont-induced alterations

in host phenotype affecting mating (or fertilization) rate are an adaptation of the endosymbiont to maintain its infection (Marshall, 2007). We believe that our model is the minimal model that captures the essence of the system studied here. However, there are still some extensions that can potentially result in qualitatively different dynamics. For example, one possible extension is to assume more than one female trait is involved in sexual conflict (e.g. Rowe *et al.*, 2003, 2005). Another would be to relax the assumptions of constant genetic variance and weak selection. We note that assuming constant genetic variances severely limits the possibility of divergence in traits (Gavrilets & Hayashi, 2005; Hayashi *et al.*, 2007). Yet another important extension is to relax the assumption that the degree of phenotypic alteration by the endosymbiont cannot evolve. This assumption means that there is no heritable variation in the degree of phenotypic alteration in endosymbiont population, which may not be a general case. Incorporating the evolution of the degree of phenotypic alteration may result in qualitatively different coevolutionary dynamics. For example, in principle, female genotypes could remain fixed and sexual conflict could drive evolutionary changes in male genotypes and the trait of endosymbionts only. Exploring these extensions is a necessary next step for advancing the theory presented here.

Acknowledgments

We thank J. Polechova, D.L. Huestis, and two anonymous reviewers for providing constructive comments on the manuscript. We thank N. Kondo for providing useful information about endosymbiont biology. This work was supported by National Institutes of Health grant GM56693 (S.G.), National Science Foundation grant DEB-0111613 (S.G.) and the Kansas Agricultural Experiment Station (contribution#08-69-J; J.L.M).

References

- Arnqvist, G. 2004. Sexual conflict and sexual selection: lost in the chase. *Evolution* **58**: 1383–1388.
- Arnqvist, G. & Nilsson, T. 2000. The evolution of polyandry: multiple mating and female fitness in insects. *Anim. Behav.* **60**: 145–164.
- Arnqvist, G. & Rowe, L. 2005. *Sexual Conflict*. Princeton University Press, Princeton, NJ.
- Birkhead, T.R. 2000. *Promiscuity*. Harvard University Press, Cambridge, MA.
- Bordenstein, S.R., O'hera, F.P. & Werren, J.H. 2001. *Wolbachia*-induced incompatibility precedes other hybrid incompatibility in *Nasonia*. *Nature* **409**: 707–710.
- Chapman, T., Liddle, L., Kalb, J., Wolfner, M. & Partridge, L. 1995. Cost of mating in *Drosophila melanogaster* females is mediated by male accessory gland products. *Nature* **373**: 241–244.
- Chapman, T., Arnqvist, G., Bangham, J. & Rowe, L. 2003. Sexual conflict. *Trends Ecol. Evol.* **18**: 41–47.
- Civetta, A. & Clark, A.G. 2000. Correlated effects of sperm competition and postmating female mortality. *Proc. Natl Acad. Sci. U.S.A.* **97**: 13162–13165.
- Gavrilets, S. 1997. Coevolutionary chase in exploiter–victim systems with polygenic characters. *J. Theor. Biol.* **186**: 527–534.
- Gavrilets, S. 2000. Rapid evolution of reproductive isolation driven by sexual conflict. *Nature* **403**: 886–889.
- Gavrilets, S. & Hayashi, T.I. 2005. Speciation and sexual conflict. *Evol. Ecol.* **19**: 167–198.
- Gavrilets, S. & Hayashi, T.I. 2006. The dynamics of two- and three-way sexual conflicts over mating. *Philos. Trans. R. Soc. B.* **361**: 345–354.
- Gavrilets, S. & Waxman, D. 2002. Sympatric speciation by sexual conflict. *Proc. Natl Acad. Sci. U.S.A.* **99**: 10533–10538.
- Gavrilets, S., Arnqvist, G. & Friberg, U. 2001. The evolution of female mate choice by sexual conflict. *Proc. R. Soc. B.* **268**: 531–539.
- Hayashi, T.I., Vose, M. & Gavrilets, S. 2007. Genetic differentiation by sexual conflict. *Evolution* **61**: 516–529.
- Hoffmann, A.A., Turelli, M. & Harshman, L.G. 1990. Factors affecting the distribution of cytoplasmic incompatibility in *Drosophila simulans*. *Genetics* **126**: 933–948.
- Holland, B. & Rice, W.R. 1998. Chase-away sexual selection: antagonistic seduction versus resistance. *Evolution* **52**: 1–7.
- Iwasa, Y., Pomiankowski, A. & Nee, S. 1991. The evolution of costly mate preferences. II. The 'handicap' principle. *Evolution* **45**: 1431–1442.
- Lande, R. 1976. Natural selection and random genetic drift in phenotypic evolution. *Evolution* **30**: 314–334.
- Lande, R. 1979. Quantitative genetic analysis of multivariate evolution, applied to brain:body size allometry. *Evolution* **33**: 402–416.
- Maklakov, A.A., Bilde, T. & Lubin, Y. 2005. Sexual conflict in the wild: elevated mating rate reduces female lifetime reproductive success. *Am. Nat.* **165**: S38–S45.
- Marshall, J.L. 2004. The *Allonemobius*–*Wolbachia* host–endosymbiont system: evidence for rapid speciation and against reproductive isolation driven by cytoplasmic incompatibility. *Evolution* **58**: 2409–2425.
- Marshall, J.L. 2007. Rapid evolution of spermathecal duct length in the *Allonemobius socius* complex of crickets: species, population and *Wolbachia* effects. *PLoS One* **2**: e720.
- Martin, O.Y. & Hosken, D.J. 2003. The evolution of reproductive isolation through sexual conflict. *Nature* **423**: 979–982.
- Partridge, L. & Hurst, L.D. 1998. Sex and conflict. *Science* **281**: 2003–2008.
- Pizzari, T. & Snook, R.R. 2003. Perspective: sexual conflict and sexual selection: chasing away paradigm shifts. *Evolution* **57**: 1223–1236.
- Rice, W.R. 1998. Intergenomic conflict, interlocus antagonistic coevolution, and the evolution of reproductive isolation. In: *Endless Forms: Species and Speciation* (D. J. Howard & S. H. Berlocher, eds), pp. 261–270. Oxford University Press, New York.
- Rice, W.R. & Holland, B. 1997. The enemies within: intergenomic conflict, interlocus contest evolution (ICE), and intraspecific Red Queen. *Behav. Ecol. Sociobiol.* **41**: 1–10.
- Rigaud, T. & Moreau, M. 2004. A cost of *Wolbachia*-induced sex reversal and female-biased sex ratios: decrease in female fertility after sperm depletion in a terrestrial isopod. *Proc. R. Soc. B.* **271**: 1941–1946.

- Rokas, A. 2000. *Wolbachia* as a speciation agent. *Trends Ecol. Evol.* **15**: 44–45.
- Rowe, L., Cameron, E. & Day, T. 2003. Detecting sexually antagonistic coevolution with population crosses. *Proc. R. Soc. B* **270**: 2009–2016.
- Rowe, L., Cameron, E. & Day, T. 2005. Escalation, retreat, and female indifference as alternative outcomes of sexually antagonistic coevolution. *Am. Nat.* **165**: S5–S18.
- Shoemaker, D.D. 1999. *Wolbachia* and the evolution of reproductive isolation between *Drosophila recens* and *Drosophila subquinaria*. *Evolution* **53**: 1157–1164.
- Turelli, M. 1994. Evolution of incompatibility-inducing microbes and their hosts. *Evolution* **48**: 1500–1513.
- Turelli, M., Hoffmann, A.A. & Mckechnie, S.W. 1992. Dynamics of cytoplasmic incompatibility and mtDNA variation in natural *Drosophila simulans* populations. *Genetics* **132**: 713–723.
- Wade, M.J. 2001. Infectious speciation. *Nature* **409**: 675–677.
- Wade, M.J. & Chang, N.W. 1995. Increased male fertility in *Tribolium confusum* beetles after infection with the intracellular parasite *Wolbachia*. *Nature* **373**: 72–74.
- Weeks, A.R., Reynolds, K.T. & Hoffmann, A.A. 2002. *Wolbachia* dynamics and host effects: what has (and has not) been demonstrated? *Trends Ecol. Evol.* **17**: 257–262.
- Wernegreen, J.J. 2004. Endosymbiosis: lessons in conflict resolution. *PLoS Biol.* **2**: 0307–0311.
- Werren, J.H. 1997. Biology of *Wolbachia*. *Annu. Rev. Entomol.* **42**: 587–609.
- Werren, J.H. & Windsor, D.M. 2000. *Wolbachia* infection frequencies in insects: evidence of a global equilibrium? *Proc. R. Soc. B* **267**: 1277–1285.
- Zeh, J.A. & Zeh, D.W. 2005. Maternal inheritance, sexual conflict and the maladapted male. *Trends Ecol. Evol.* **21**: 281–286.

Received 4 June 2007; revised 19 July 2007; accepted 2 August 2007

Appendix

Analysis of the dynamics of \bar{x} and \bar{y}

We can analyse the coevolutionary dynamics between \bar{x} and \bar{y} by focusing on the dynamics of displacement \bar{z} (given by $\bar{z} = \bar{y} - \bar{x}$). From eqns (9a) and (9b), the difference in the \bar{z} between subsequent generations is

$$\begin{aligned} \Delta\bar{z} &= \Delta\bar{y} - \Delta\bar{x} \\ &= p[V_y b - V_x a(\Psi_I - P_{\text{opt}})]\Psi_{yI} \\ &\quad + (1-p)[V_y b - V_x a(\Psi_U - P_{\text{opt}})]\Psi_{yU} \\ &= pI\Psi_{yI} + (1-p)U\Psi_{yU}, \end{aligned} \quad (A1)$$

where $I = V_y b - V_x a(\Psi_I - P_{\text{opt}})$ and $U = V_y b - V_x a(\Psi_U - P_{\text{opt}})$.

Case 1: a monotonically increasing compatibility function

First, as a simple example, we assume a monotonically increasing compatibility function in which increasing \bar{z} always increases compatibility (e.g. an S-shaped compatible function). This 'monotonically increasing compatibility' means that Ψ_{yI} and Ψ_{yU} are always positive, and it enables us to analytically show that the qualitative

outcome of the dynamics of \bar{z} depends on the sign of $V_y b - V_x a(1 - P_{\text{opt}})$. If sexual selection in males is sufficiently strong relative to that in females [precisely, $V_y b - V_x a(1 - P_{\text{opt}}) > 0$], the signs of $I\Psi_{yI}$ and $U\Psi_{yU}$ are always positive. Thus, \bar{z} always increases and mating rate becomes one (corresponding to the case shown in Fig. 2a–c). If sexual selection in males is not sufficiently strong relative to that in females [precisely, $V_y b - V_x a(1 - P_{\text{opt}}) < 0$], the signs of I and U depend on \bar{z} . In the range of $\Psi_I < P_{\text{opt}} + bV_y/aV_x < \Psi_U$, the signs of $I\Psi_{yI}$ and $U\Psi_{yU}$ are opposite. Then $\Delta\bar{z}$ becomes zero in a point in the range of \bar{z} that satisfies $\Psi_I \leq P_{\text{opt}} + bV_y/aV_x \leq \Psi_U$ (corresponding to the case shown in Fig. 2d–f), depending on the equilibrium value of p that satisfies eqn (11a). [Note that \bar{z} approaches the value of \bar{z} satisfying $\Psi_U = P_{\text{opt}} + bV_y/aV_x$ when $p = 0$ (Gavrilets *et al.*, 2001).] When $P_{\text{opt}} + bV_y/aV_x < \Psi_I < \Psi_U$, \bar{z} decreases into the value of \bar{z} satisfying $\Psi_I \leq P_{\text{opt}} + bV_y/aV_x \leq \Psi_U$ (or approaches to the value satisfying $\Psi_U = P_{\text{opt}} + bV_y/aV_x$ if no infection is maintained).

Case 2: a symmetrical unimodal compatibility function

Here, we assume a symmetrical unimodal compatibility function in which the compatibility reaches maximum when the male phenotype equals the female phenotype (e.g. a compatible function with quadratic form). We also assume $c > 0$. [These assumptions mean that Ψ_{yI} and Ψ_{yU} have opposite signs ($\Psi_{yI} > 0$ and $\Psi_{yU} < 0$) in the range of $0 < \bar{z} < \bar{c}$, and have the same sign in the range of $\bar{z} < 0$ or $\bar{z} > \bar{c}$.] The qualitative outcome of \bar{z} depends on the sign of $V_y b - V_x a(1 - P_{\text{opt}})$. First, suppose the case in which sexual selection in males is sufficiently strong relative to that in females [precisely, $V_y b - V_x a(1 - P_{\text{opt}}) > 0$]. When $0 < \bar{z} < c/2$, I and U are always positive and thus the signs of $I\Psi_{yI}$ and $U\Psi_{yU}$ are opposite. Then, $\Delta\bar{z}$ becomes zero in a point in the range of $0 \leq \bar{z} < c/2$ (corresponding to the case shown in Fig. 1a–c), depending on the equilibrium value of p that satisfies eqn (11a). [Note that $\Delta\bar{z}$ becomes zero at $\bar{z} = 0$ when $p = 0$ (Gavrilets, 2000). When $\bar{z} \geq 2/c$, infection is not maintained (i.e. $p = 0$) because condition (13) is not satisfied.] When $\bar{z} < 0$, \bar{z} increases to the range of $\bar{z} \geq 0$.

If sexual selection in males is not sufficiently strong relative to that in females [precisely, $V_y b - V_x a(1 - P_{\text{opt}}) < 0$], the sign of I and U depend on \bar{z} . In the range of $\Psi_I \leq P_{\text{opt}} + bV_y/aV_x \leq \Psi_U$ and $\bar{z} < 0$, the signs of $I\Psi_{yI}$ and $U\Psi_{yU}$ are opposite. Then $\Delta\bar{z}$ becomes zero in a point in the range of $\bar{z} < 0$ (corresponding to the case shown in Fig. 1d–f), depending on the equilibrium value of p that satisfies eqn (11a). [Note that $\Delta\bar{z}$ asymptotically approaches to zero where \bar{z} satisfies $\Psi_U = P_{\text{opt}} + bV_y/aV_x$ when $p = 0$ (Gavrilets, 2000).] In the range of $\Psi_I \leq P_{\text{opt}} + bV_y/aV_x \leq \Psi_U$ and $0 \leq \bar{z} \leq c/2$, \bar{z} increases into the range of $\bar{z} \geq c/2$ where infection cannot be maintained (i.e. p becomes zero). In the range of $P_{\text{opt}} + bV_y/aV_x < \Psi_I < \Psi_U$ and $\bar{z} < 0$, \bar{z} decreases into the value

satisfying $\Psi_I \leq P_{\text{opt}} + bV_y/aV_x \leq \Psi_U$ (or approaches to the value satisfying $\Psi_U = P_{\text{opt}} + bV_y/aV_x$ if no infection is maintained). In the range of $P_{\text{opt}} + bV_y/aV_x < \Psi_I < \Psi_U$ and $0 \leq \bar{z} \leq c/2$, the signs of $I\Psi_{yI}$ and $U\Psi_{yU}$ are opposite. Then $\Delta\bar{z}$ can be zero in a point in the range of $0 \leq \bar{z} \leq c/2$, depending on the equilibrium value of p . Our numerical simulations suggest that this equilibrium is unstable and \bar{z} eventually increases to the range

$\bar{z} \geq c/2$ (in which no infection is maintained) or decreases to the range $\bar{z} < 0$ (the case discussed above).

The complexity of the dynamic equations (eqns 9a–9c) makes it difficult to make further analytical examination of the system. Our numerical simulations to show the combined dynamics of p and \bar{z} were given in the main body of the paper.